Res. Rep. Fac. Eng. Mie Univ., Vol. 6, pp. 51-62(1981)

Original Paper

Consideration on the Mechanism of Reheat Cracking of Cr-Mo Steels — Mechanism of Grain Boundary Embrittlement by Carbide Precipitation —

Koreaki TAMAKI and Jippei SUZUKI
(Department of Mechanical and Materials Engineering)

(Received September 16, 1981)

The following points are introduced in order as concerned to reheat cracking sensitivity and crack producing mechanism. i) Reheat cracking sensitivity of various Cr-Mo steels was quantitatively compared using critical stress for producing cracking (σAW-crit). ii) There was a chemical composition field in which cracking sensitivity is very high (Field III). iii) In such the field, M_2C carbide generally precipitates. It will play an important role to produce the cracking. iv) But the grain strengthening effect of M_2C was not so much decisive to crack formation, as was expected from the precipitation hardening hypothesis. v) Then the authors propose a new type of phosphorus-embrittling hypothesis which can explain the mechanism of phosphorus segregation caused mainly by M_2C precipitation.

1. Introduction

Reheat cracking (stress relief cracking; SR cracking) occurs at grain boundary of prior-austenite in heat affected zone (HAZ) of Cr-Mo steels when the welded steels are reheated through 550°C to 600°C for stress relief annealing. The Cr-Mo steels in which M_2C (Mo_2C type carbide) precipitates are most sensitive to reheat cracking.

There have been proposed two hypotheses for crack producing mechanism:

i) Precipitation hardening hypothesis,[1)]

ii) Phosphorus-embrittling hypothesis.[2)]

The former explains that the ferrite grain is strengthened by the precipitation of carbides, such as M_2C, and the grain becomes difficult to deform and therefore the grain boundary sliding is forced to occur until it produces grain boundary cracking.

The latter explains that the grain boundary becomes brittle by the segregation of some impulrty elements, such as phosphorus. But it is not yet

explained by the hypothesis whether M_2C precipitation relates the segregation or not.

In this report, the authors have discussed at first the precipitation hardening hypothesis, and confirmed that this hypothesis alone can not explain completely the various phenomena of reheat cracking.

Then the authors have proposed a new mechanism that carbides, such as M_2C, embrittle the grain boundary and, at the same time, they strengthen the grain interior. This mechanism includes both the hypotheses above mentioned, and is developed by the authors on the basis of the information about the solid solubility of phosphorus in ferrite, and the precipitation behaviors of carbide and phosphide.

2. Reheat cracking sensitivity of Cr-Mo steels

The authors have measured the critical stress for producing reheat cracking, ÓAW-crit by the cracking test using the implant method.[3] On the basis of the results on the specimens of Table 1, the Cr-Mo contents diagram on which the contour lines of ÓAW-crit were drawn was proposed as shown in Fig.1.[4)5)]

Table 1 Chemical compositions of Cr-Mo steels wt%

series	No	C	P	Cr	Mo
A	A-0	0.20	0.02	0.00	0.27
	A-1	0.21	0.02	0.49	0.25
	A-2	0.20	0.02	1.03	0.29
	A-3	0.19	0.02	1.83	0.27
B	B-0	0.12	0.020	0.04	0.51
	B-1	0.12	0.018	0.58	0.54
	B-2	0.12	0.016	1.10	0.53
	B-3	0.13	0.018	1.83	0.52
	B-4	0.14	0.017	2.57	0.53
	B-5	0.14	0.018	5.32	0.51
C	C-0	0.13	0.021	0.01	0.96
	C-1	0.14	0.018	0.46	0.92
	C-2	0.14	0.020	1.14	0.96
	C-3	0.13	0.021	1.44	0.91
	C-4	0.13	0.019	2.03	0.93
	C-5	0.14	0.021	4.27	0.95
D	D-0	0.20	0.02	0.01	1.43
	D-1	0.18	0.02	0.91	1.51
	D-2	0.20	0.02	1.83	1.44
	D-3	0.19	0.02	2.73	1.57

The others : Si 0.3～0.5% Mn 0.9～1.3% S 0.02%

The chemical compositions of Cr-Mo steels may be divided into four fields according to the cracking sensitivity for the convenience of explanation as shown in Fig.1-(b).

Field I ; The field of lower chromium and molybdenum contents. The cracking sensitivity is very low in this field.

Field IIa ; The field, in which the cracking sensitivity increases remarkably with the increase of chromium content up to about 1.1%. Molybdenum effect of increasing the sensitivity is also large.

Field IIb ; The field, in which the cracking sensitivity decreases gradually with the increase of chromium content from about 1.1%.

Field III ; The field, in which the cracking sensitivity is very high.

The chemical compositions of the various industrial Cr-Mo steels including HT80 are also shown in the figure.

3. Relation between carbide precipitation and cracking sensitivity

Carbide types which precipitate during tempering (reheating) of various Cr-Mo steels were determined by X-ray analyses on electrolytically extracted carbide. The result is shown in Table 2. The carbide phase change with increasing tempering time at 600°C can be summerized as follows.*

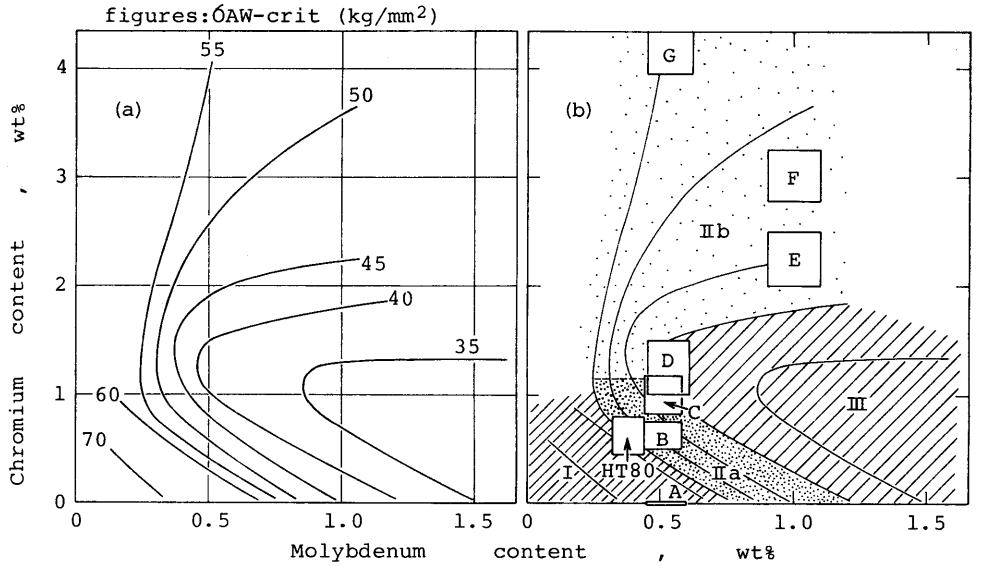

Fig.1 Contour lines of critical restraint stress (ΔAW-crit) shown in the Cr-Mo contents diagram

note : A;$\frac{1}{2}$Mo steel, B;$\frac{3}{4}$Cr-$\frac{1}{2}$Mo steel, C;1Cr-$\frac{1}{2}$Mo steel, D;1$\frac{1}{4}$Cr-$\frac{1}{2}$Mo steel, E;2$\frac{1}{4}$Cr-1Mo steel, F;3Cr-1Mo steel, G;5Cr-$\frac{1}{2}$Mo steel

Lower chromium content : $M_3C \longrightarrow M_2C$

Medium chromium content : $\begin{cases} M_3C \longrightarrow M_2C \\ M_3C \longrightarrow M_7C_3 \end{cases}$

High chromium content : $M_3C \longrightarrow M_7C_3 \longrightarrow M_{23}C_6$

Carbide types precipitated by tempering for 1 and 24 hr at 600°C are shown in Cr-Mo contents diagram, as in Fig.2. M_2C precipitates in the field of about 0.5%Mo and 0 to 2%Cr (shaded field). Such the field corresponds to the field III of Fig.1 in which the cracking sensitivity becomes the maximum, except for the lower chromium-molybdenum side.

Table 2 Carbide types present in Cr-Mo steels tempered at 600°C confirmed by X-ray diffraction

	steel (%)			Carbide types in steel tempered for :				
No	C	Cr	Mo	0.24 hr	1 hr	5 hr	24 hr	100 hr
B-0	0.12	0.04	0.51	M_3C	M_3C	M_3C	M_3C+M_2C	M_3C+M_2C
B-1	0.12	0.58	0.54	M_3C	M_3C	M_3C	M_3C+M_2C	M_3C+M_2C
B-2	0.12	1.10	0.53	M_3C	M_3C	M_3C	$M_2C+M_7C_3$	M_7C_3
B-3	0.13	1.83	0.52	M_3C	M_3C	$M_3C+M_7C_3$	M_7C_3	M_7C_3
B-4	0.14	2.57	0.53	M_7C_3	M_7C_3	$M_7C_3+M_{23}C_6$	$M_7C_3+M_{23}C_6$	$M_7C_3+M_{23}C_6$
B-5	0.14	5.32	0.51	M_7C_3	M_7C_3	$M_7C_3+M_{23}C_6$	$M_7C_3+M_{23}C_6$	$M_7C_3+M_{23}C_6$
C-0	0.13	0.01	0.96	M_3C	M_3C+M_2C	M_3C+M_2C	M_3C+M_2C	M_3C+M_2C
C-1	0.14	0.46	0.92	M_3C	M_3C+M_2C	M_3C+M_2C	M_3C+M_2C	M_3C+M_2C
C-2	0.14	1.14	0.96	M_3C	M_3C+M_2C	M_3C+M_2C	M_3C+M_2C	$M_3C+M_2C+M_7C_3$
C-3	0.13	1.44	0.91	M_3C	$M_3C+M_7C_3$	$M_3C+M_7C_3$	$M_7C_3+M_2C$	$M_2C+M_7C_3$
C-4	0.14	2.03	0.93	M_3C	M_3C	$M_3C+M_7C_3$	$M_3C+M_7C_3+M_2C$	$M_7C_3+M_{23}C_6$
C-5	0.14	4.27	0.95	$M_3C+M_7C_3$	$M_7C_3+M_{23}C_6$	$M_7C_3+M_{23}C_6$	$M_{23}C_6$	$M_{23}C_6$

* M_3C : Fe_3C type carbide containing Mo and Cr as solid solution. M_2C : Mo_2C type carbide containing Cr and Fe. M_7C_3 : Cr_7C_3 type carbide containing Mo and Fe. $M_{23}C_6$: $Cr_{23}C_6$ type carbide containing Mo and Fe.

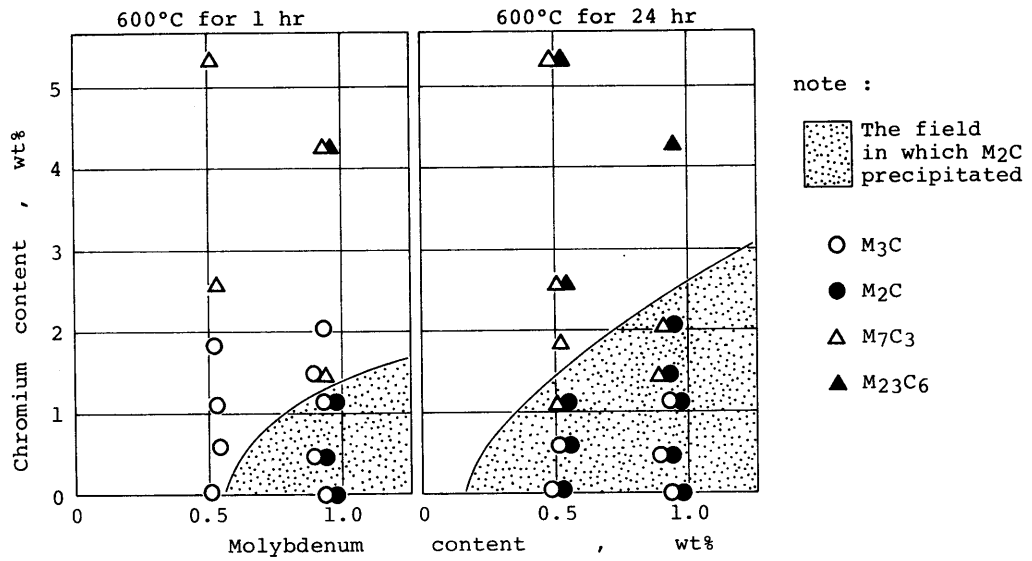

Fig.2 Carbide types present in Cr-Mo steels tempered at 600°C confirmed by X-ray diffraction

4. Relation between secondary hardening and reheat cracking

Hardness at each tempering temperature is shown for the specimens of 0 to 4%Cr and 1%Mo, as Fig.3. Carbide types at each temperature are also shown in the figure. The data concerning to secondary hardening are shown in Table 3. These results can be summerized from the point of view of M_2C precipitation as follows:

i) Although the increment of hardness caused by M_2C precipitation is larger than that by M_7C_3 precipitation, it is almost the same as that by $M_{23}C_6$ precipitation.

ii) The maximum hardness value brought by M_2C is rather small as compared to those by M_7C_3 and $M_{23}C_6$.

From such the results, it will be concluded that the hardness itself at secondary hardening stage can not be directly connected to the cracking sensitivity.

The specimen of 0.46%Cr and 0.92%Mo in which M_2C precipitates was used for the measurement at high temperature. The specimen was oil quenched from 950°C, and then heated at the rate of 400°C/hr up to 350°C and hardness was measured

Table 3 Secondary hardening temperature and increase of hardness of tempered Cr-1%Mo steels

steel	wt%Cr	Temperature (°C) at beginning	Temperature (°C) at Hv-max	Hardness Hv-max	Hardness increase of Hv	Carbide at 600°C for 1 hour
C-1	0.46	480	550	350	20	M_2C + M_3C
C-2	1.14	450	500	390	5	M_2C + M_3C
C-4	2.03	450	500	410	5	M_3C + M_7C_3
C-5	4.27	400	500	420	20	M_7C_3 + $M_{23}C_6$

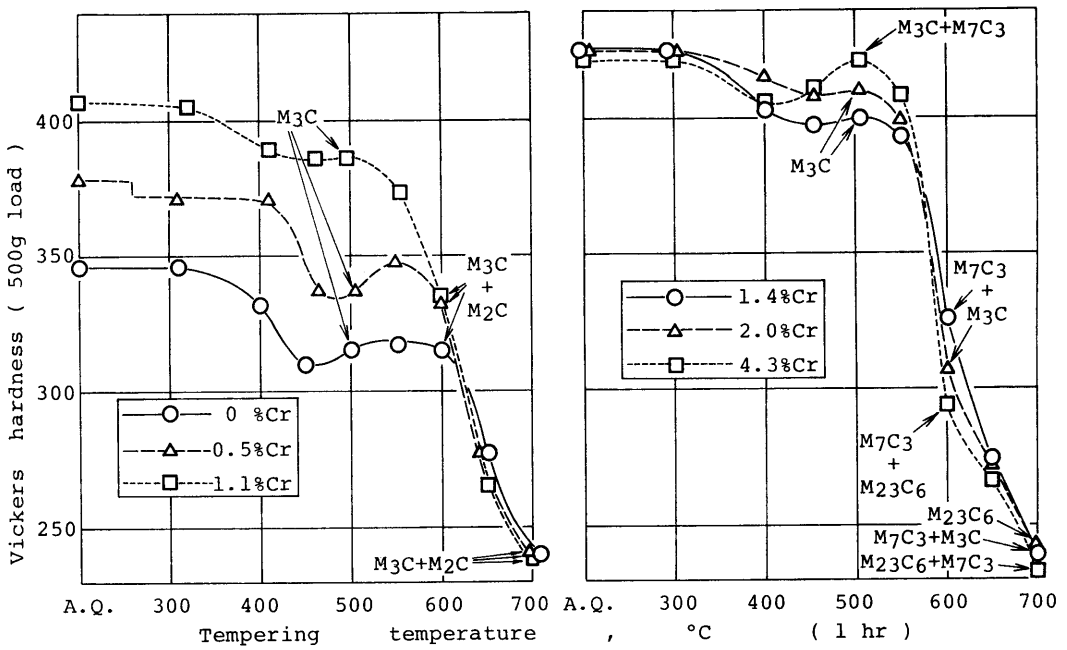

Fig.3 Effect of chromium on the hardness of tempered 1%Mo steels
note : Carbide types shown in the figure were determined by X-ray diffraction on extracted carbides. A.Q.;as-quenched

15 min later at this temperature, and then at 400, 450,·····°C by the same way, respectively. The result is shown by the mark ○ in Fig.4. Hardness measured at room temperature is also shown in the figure by the mark ● .

There can be seen the delay of softening in the hardness curve of high temperature in the temperature range of about 480°C to 600°C. But the secondary hardening phenomenon, which was usually observed in the hardness curve at room temperature, can not be recognized.

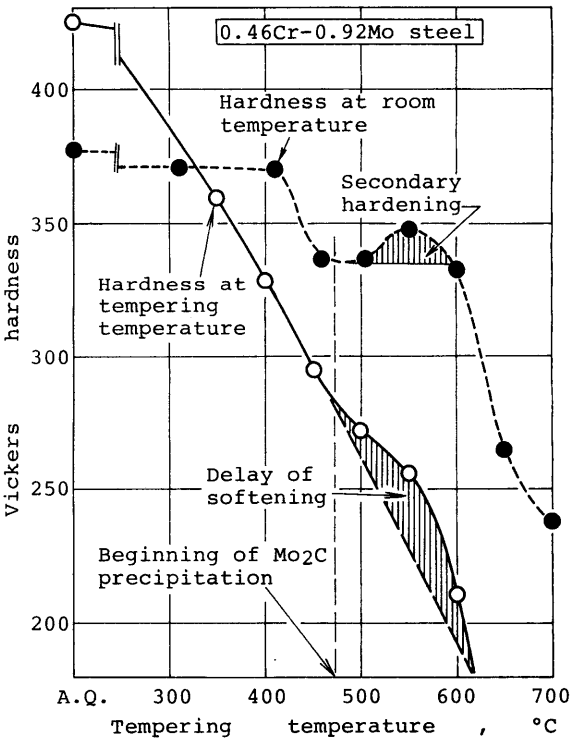

Fig.4 Hardness at each tempering temperature obtained by the measurement at high temperature (○ mark)
note: A.Q.;as-quenched

5. Comment on the precipitation hardening hypothesis

The precipitation hardening hypothesis will require the following conditions.

i) The grain interior is hardened.
ii) The grain boundary is embrittled.
iii) Both the phenomena i) and ii) should occur in a same temperature range.

If the sources of grain strengthening and grain boundary embrittling are different each other, it is generally difficult to satisfy the condition iii). That is, the temperature range in which the maximum embrittlement can not always fall on the range in which enough strength is still maintained, because the strengthened condition can not continue over a wide temperature range, as pointed out in the above section.

On the contrary, if the source of the grain boundary embrittlement is same as that of the grain strengthening, namely M_2C precipitation, the condition iii) is necessarily satisfied.

On the basis of such the considerations, the authors propose " The mechanism of grain boundary embrittlement by carbide precipitation " .

6. Mechanism of grain boundary embrittlement by carbide precipitation

The authors suppose the following sequence of crack forming process.

Stage I : Phosphorus segregates at the austenite grain boundary when HAZ transforms from δ-ferrite to austenite during cooling stage after welding, because the solubility of phosphorus in austenite is much smaller than in δ-ferrite.[6)7)] Some quantity of phosphide may precipitate at the segregating zone.

Stage II : At the lower reheating temperature, phosphide additionally precipitates at the prior-austenite grain boundary (PAGB), because solid solubility of phosphorus in ferrite is limited by molybdenum in solid solution.

Stage III : At the higher reheating temperature, M_2C precipitates instead of M_3C. At this stage, the molybdenum concentration of ferrite is decreased by the formation of molybdenum carbide, M_2C. Consequently, the solubility of phosphorus is increased. Then the phosphide previously presented at PAGB dissolves and phosphorus concentration at PAGB will increase remarkably. At this stage, reheat cracking will occur at PAGB, if restraint stress is large enough.

6.1 Solubility of phosphorus in α-iron in Fe-Cr-Mo-P system

Solid solubility of phosphorus in Fe-Cr-Mo-P quarternary system at 600°C was estimated from the experimental data of those of Fe-Cr-P and Fe-Mo-P ternary systems (Fig.5-(a) and (b)).

At first, the solubility at 600°C was estimated for both ternary systems

by the following formula, as shown in Fig.5-(c) and (d).

$$\ln x = C - \Delta Q/RT$$

where, x is the solubility of phosphorus (at%), ΔQ is the heat of dissolution of phosphide (cal/mol).

Next, chromium or molybdenum contents which give the solubility values of 0.005,0.01,0.02,·····(wt%) were plotted on abscissa and ordinate, respectively.

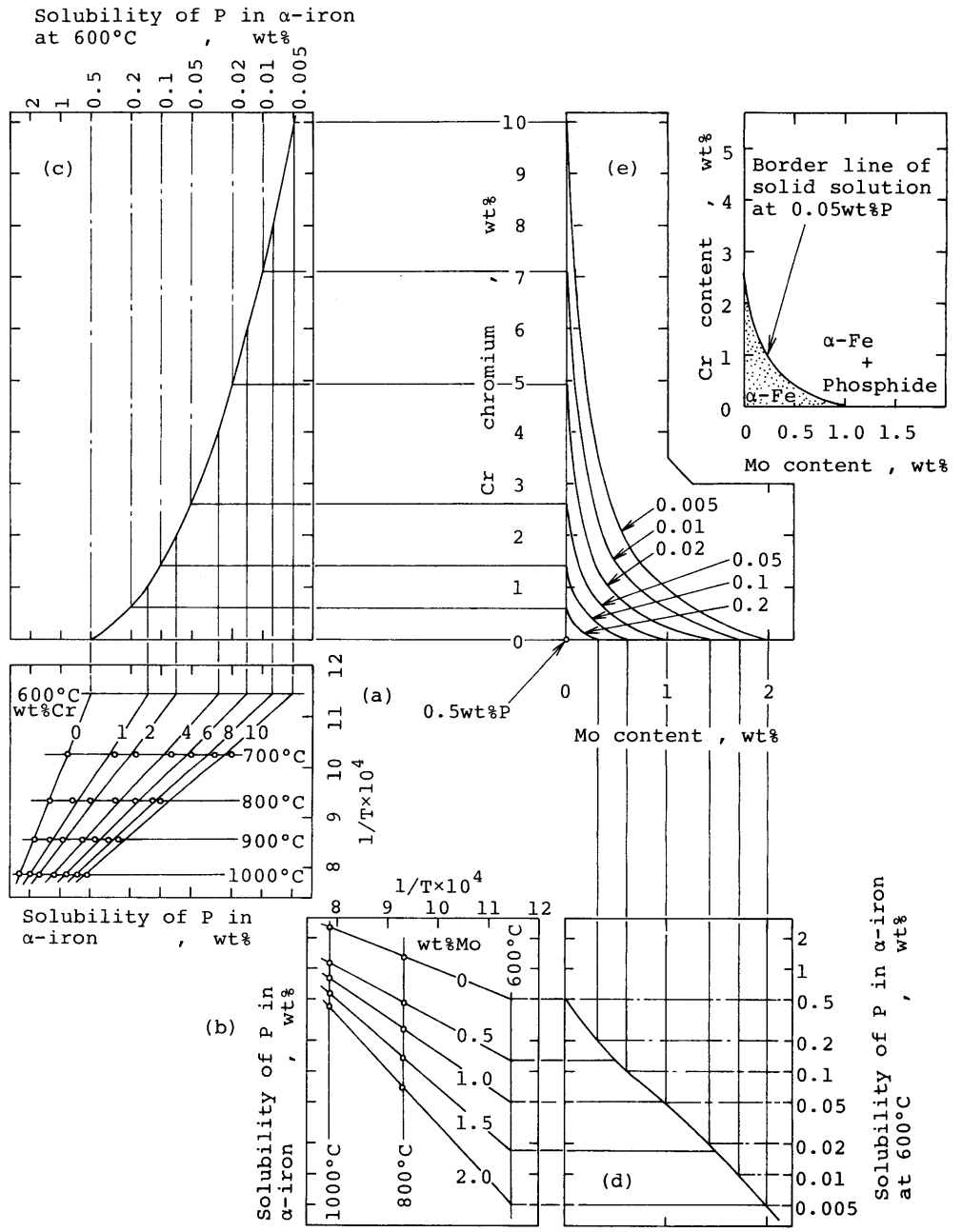

Fig.5 Estimation of the solubility of Phosphorus in α-Fe of Fe-Cr-Mo-P system from the data of Fe-Cr-P and Fe-Mo-P systems

The same values on both axes were bound by curved lines, as shown in Fig.5-(e). Those curves are convex shape according to that the mutual action between both elements will be expected towards decreasing the solubility. It must be mentioned here that the solubility curves in the figure are only qualitative ones to be used for the explanation in the following section.

The figure shows that the solubility of phosphorus, Ps decreases logarithmically with the increase of molybdenum and chromium contents of the alloy.

6.2 Increase of phosphorus solubility by carbide precipitation

The solubility of phosphorus becomes larger than that given by Fig.5, when molybdenum carbide precipitates, and therefore molybdenum concentration of ferrite matrix decreases. And then, phosphorus concentration in ferrite, [P] increases according to the dissolution of phosphide into ferrite matrix. The increment of [P] will be determined by the following factors:

i) Phosphorus content of steel, P_B

ii) Ps value which is determined by Cr-Mo contents of steel

The increment of [P] is discussed here on the typical combinations of Ps value and P_B=0.02 wt%.

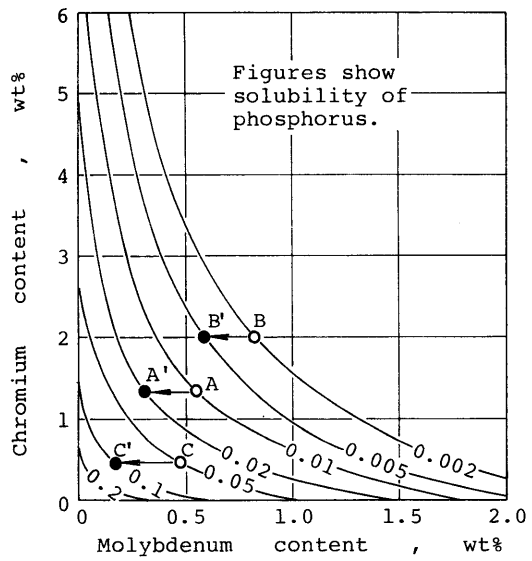

Fig.6 Increase of solid solubility of phosphorus induced by the decrease of soluble molybdenum concentration

note: o Original solute concentration (same as that bulk steel)

● Solute concentration after the precipitation of molybdenum carbide

(a) P_B slightly larger than Ps

In the case of a steel has the chemical composition of the point A in Fig.6, 0.01%P dissolves and remaining 0.01%P precipitates as phosphide when molybdenum carbide does not precipitate.

Then next, a certain part of molybdenum in ferrite is consumed by the formation of molybdenum carbide, and it decreases to, for example, the point A'. Because the Ps value of the point A' is 0.02%, 0.01%P which has previously precipitated dissolves into ferrite matrix. As the result of the "re-dissolving reaction", the dissolved phosphorus is purged at PAGB where phosphide has previously presented. And therefore the concentration of phosphorus at PAGB increases remarkably. Such the chemical composition field will correspond to the field Ⅲ and Ⅱa in Fig.1.

(b) P_B very much larger than Ps

In the case that a steel has the chemical composition of the point B in Fig.6, and P_B is very much larger than Ps (=0.002%), dissolved phosphorus does not so much increase when the carbide precipitates. Phosphorus segregation at PAGB will smaller in this steel. Such the chemical composition field will correspond to the field IIb in Fig.1.

(c) P_B smaller than Ps

In the case that a steel has the chemical composition of the point C in Fig.6, and P_B is smaller than Ps (=0.05%), all of the phosphorus dissolves in ferrite even though before the carbide precipitates. Phosphorus segregation will not occur in this steel. Such the chemical composition field will correspond to the field I in Fig.1.

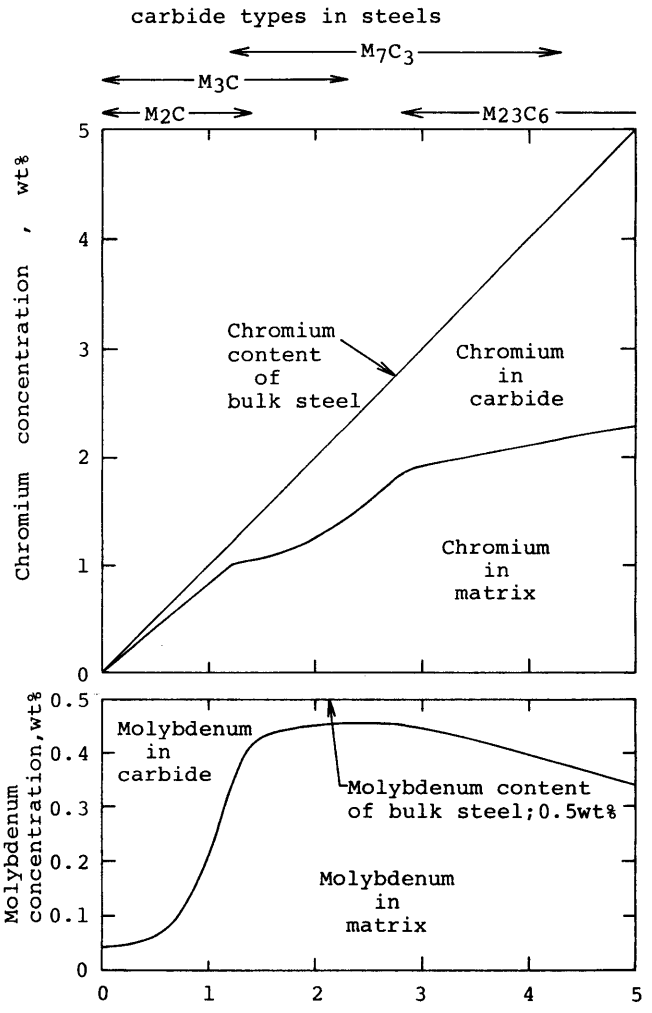

Fig.7 Molybdenum and chromium concentrations in ferrite after carbide precipitation 0.5wt%Mo, 0～5wt%Cr steels

6.3 A trial calculation of the increment of [P]

Increment of [P], that is [⊿P], was calculated tentatively on a series of 0 to 5%Cr-0.5%Mo steels.

Molybdenum and chromium concentrations in ferrite and carbide phases were estimated by the data of carbide[8)9)], as shown in Fig.7.

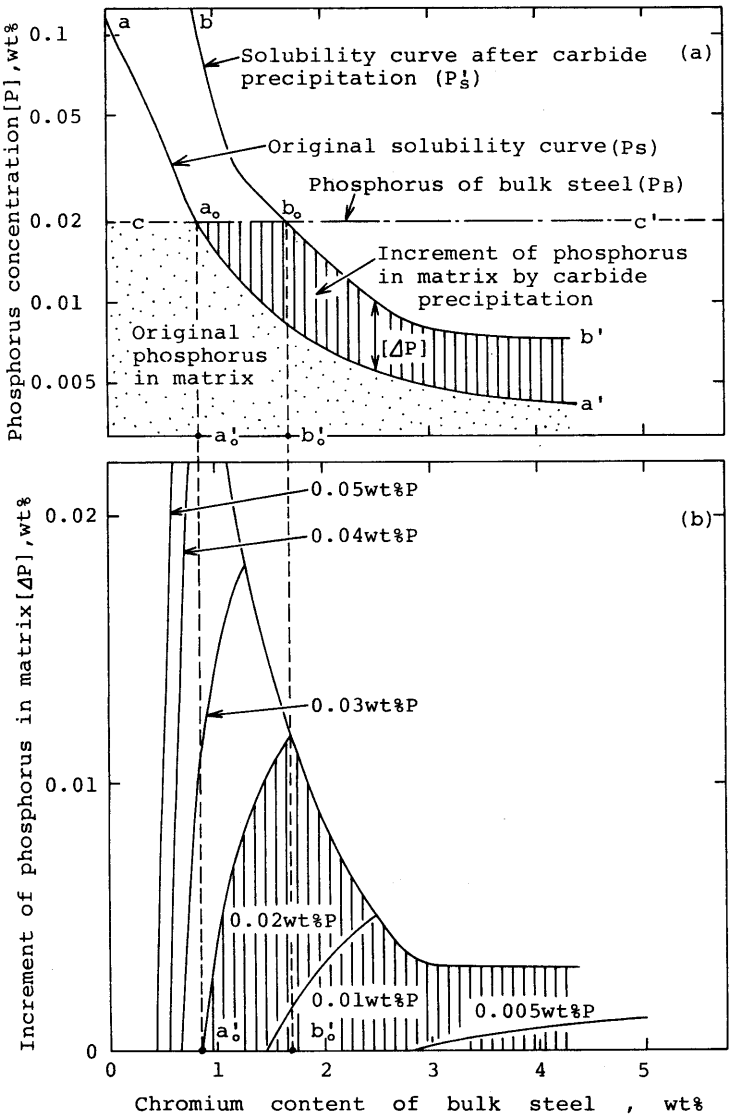

Fig.8 Increase of soluble phosphorus concentration caused by carbide precipitation
0.5wt%Mo, 0～5wt%Cr steels

At first, Ps value is directly read from Fig.6. Ps value in relation to chromium content is shown as aa' line in Fig.8-(a). The aa' line intersects cc' line, which corresponds P_B, at the point a_o, and phosphide will precipitate on the right hand side of a_oa' line.

Next, Ps' value, which is the phosphorus solubility after carbide precipitates, is read from Fig.6 using the values of molybdenum and chromium concentrations in ferrite in Fig.7, as bb' line of Fig.8-(a). Phosphide will precipitate on the right hand side of b_ob' line.

After carbide precipitation, [P] will increase as much as the difference of the value on a_ob_ob' and a_oa' lines.

Fig.8-(b) shows [ΔP] in relation to chromium content of steel. It can be seen from the figure that:

i) [ΔP] increases with the increase of chromium content from the chromium content of which P_B equals Ps (a_o' in the figure).

ii) [ΔP] is the maximum at the chromium content of which Ps' equals to P_B (b_o' in the figure).

iii) [ΔP] decreases with the increase of chromium content when it becomes larger than b_o'.

The effect of P_B on [ΔP] is also shown for 0.005 to 0.05%P in Fig.8-(b). Such the result explains that:

i) [ΔP] increases remarkably with the increase of P_B on the steels of lower chromium content, but does little on the steel of higher chromium content.

ii) The higher is P_B, the lower is the chromium content which gives the maximum [ΔP].

7. Conclusion

Reheat cracking sensitivity of Cr-Mo steels was discussed from the point of view of carbide precipitation and solubility of phosphorus. And the authors proposed the following mechanism of phosphorus segregation which is followed by crack formation.

(1) Phosphorus segregation at the PAGB can be explained by the process that the carbide (such as M_2C) precipitation causes the increase of solubility of phosphorus, and as the result of it, phosphide which has previously precipitated at the PAGB re-dissolves into ferrite matrix.

(2) Such the reaction will most remarkably occur in the steels of which P_B is slightly larger than Ps.

(3) Such the effect will be little in the steels of higher chromium and molybdenum contents and therefore the solubility is very small, and also in the steels of lower chromium and molybdenum contents and the solubility is very large.

Acknowledgments

The present investigation has been supported by The Grant-in-Aid for Scientific Research of The Ministry of Education and Culture, Japan.

The authors wish to thank Professor Taira Okamoto and Associate Professor Masahiko Simada of The Institute of Scientific and Industrial Research, Osaka University for their kind support on the measurement of high temperature hardness.

The authors wish to thank the students of Mie University, Messrs. Tadashi Iizuka, Ichiro Kato, Yoshimoto Nakaseko, Yasuyuki Hakamada, Yasunari Suzuki, Hideaki Yoneyama, Akira Matumoto, Tatuhiro Yamashita, Takao Asai, Kazuo Kodama and Hisao Horibe for their cooperation.

References

1) Y.Ito, M.Nakanishi : J.Japan Welding Soc., 40-12(1971), 1261-1266 [in Japanese]
2) Y.Nakao, T.Nishiyama : J.Japan Welding Soc., 49-12(1980), 835-839 [in Japanese]
3) K.Tamaki, J.Suzuki : Res.Rep.Fac. Eng.Mie Univ., Vol.5(1980), 49-58
4) K.Tamaki, J.Suzuki, M.Kojima : The combined influences on chromium and molybdenum on stress relief cracking, International Inst. Welding, Doc.IX-1112-79, (1979)
5) K.Tamaki, J.Suzuki, Y.Nakaseko : Effect of molybdenum carbide on reheat cracking sensitivity of Cr-Mo steels, International Inst. Welding, Doc.IX-1159-80, (1980)
6) H.Kaneko, T.Nishizawa, K.Tamaki : J.Japan Inst. Metals, 29-2(1965), 159-165 [in Japanese]
7) H.Kaneko, T.Nishizawa, K.Tamaki, A.Tanifuji : J.Japan Inst. Metals, 29-2(1965), 166-170 [in Japanese]
8) K.Bungardt, E.Kunze, E.Horn : Arch. Eisenhutt., 29(1958), 192-203
9) T.Sato, T.Nishizawa, K.Tamaki : Trans. Japan Inst. Metals, 3-4(1960), 196-202